Structure of the solar chromosphere

Sami K. Solanki

Max-Planck-Institut für Sonnensystemforschung, Max-Planck-Str. 2, 37191
Katlenburg-Lindau, Germany, email: solanki@mps.mpg.de

Abstract. The chromosphere is an intriguing part of the Sun that has stubbornly resisted all attempts at a comprehensive description. Thus, observations carried out in different wavelength bands reveal very different, seemingly incompatible properties. Not surprisingly, a debate is raging between supporters of the classical picture of the chromosphere as a nearly plane parallel layer exhibiting a gentle temperature rise from the photosphere to the transition region and proponents of a highly dynamical atmosphere that includes extremely cool gas. New data are required in order settle this issue. Here a brief overview of the structure and dynamics of the solar chromosphere is given, with particular emphasis on the chromospheric structure of the quiet Sun. The structure of the magnetic field is also briefly discussed, although filaments and prominences are not considered. Besides the observations, contrasting models are also critically discussed.

1. Introduction: Chromospheric structure

The solar chromosphere is traditionally defined as the layer, lying between the photosphere and the transition region, where the temperature first starts to rise outwards. The lower boundary in this definition is formed by the temperature minimum layer. The upper boundary is less clearly marked, however, with a temperature around $1-2\times10^4$ K generally being prescribed. More recently, the concept of a gradually increasing temperature in the chromosphere has been questioned. An alternative, rough definition of the chromosphere is the location of the non-photospheric gas (i.e. gas lying above the layers at which convective overshoot dominates proceedings) at temperatures roughly below 10^4 K. These simple definitions do not do justice to the chromosphere's many faces. Some of these faces have to do with the different solar features with which this gas is associated. These are often determined by the magnetic structure: Basically, we distinguish between the active and the quiet chromosphere. The former includes structures such as sunspots and plages, flare ribbons, eruptions and surges; the latter includes features such as network and internetwork, Hα-grains, quiescent prominences and filaments, spicules, cool CO-clouds, 3 min oscillations, shock waves etc. In view of this variety, other, nonrigorous definitions are also worth considering. For example, the chromosphere is the layer at which the magnetic field and waves become energetically important in a global sense, or where NLTE effects begin to dominate line formation, or which produces the flash spectrum during eclipses (i.e. basically the layer in which the Hα line is formed).

The very large range of structures and the inhomogeneity of the chromosphere are best revealed when it is observed at different wavelengths, from the EUV to the radio domain. For example, plages are best seen in EUV emission lines, e.g. O I 110 nm, or He I 50.4 nm, or in strong lines at longer wavelengths, such as Mg I h and k, or Ca II H and K. Sunspots are only seen in radiation that samples the lower chromosphere (thus the EUV He II lines show them as bright structures), spicules and surges are best seen in the Hα line, which also shows prominent fibrils and grains. As the name says, the cool CO-clouds are visible practically only in the fundamental ro-vibrational bands of CO at
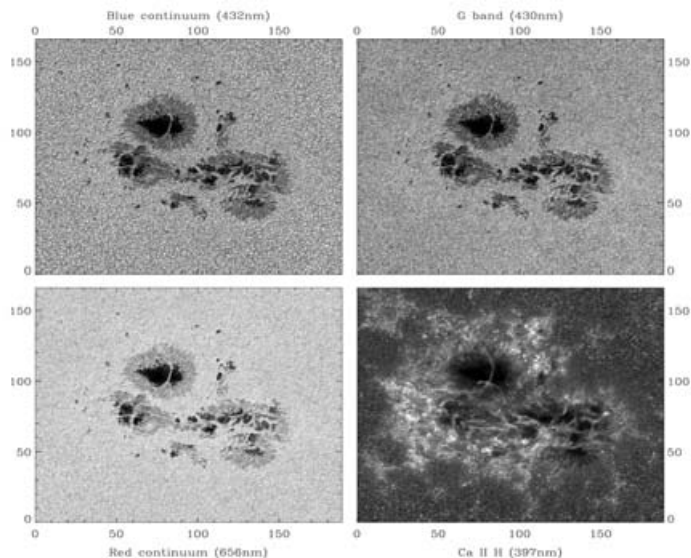
Figure 1. AR 10375 imaged with the Dutch Open Telescope in the blue continuum (upper left), the G-band (upper right), the red continuum (lower left) and the core of the Ca II H line. Figure courtesy of P. Sütterlin and R.J. Rutten.

around 4.7μm. The magnetic field in the chromosphere is made visible with polarimetry in strong spectral lines, such as Hβ, Na D, but also in the nearly optically thin He I 1083 nm line. Finally, a more holistic picture of the dynamic and inhomogeneous quiet chromosphere may be provided by sub-mm and mm data. The diversity of identities revealed by the chromosphere demonstrates the acute need to study it over a large range of wavelengths. This makes the chromosphere an ideal structure to be discussed in the context of a conference on multi-wavelength investigations of solar activity.

Fig. 1 shows a comparison between three photospheric images of active region AR 10375 and a chromospheric image in the core of the Ca II K line (bottom right frame). Note the significantly larger contrast in the Ca II K image of the magnetic features (plage and network).

In Fig. 2 a spectrum recorded by Ayres (2002) with the spectrograph slit crossing the limb of the Sun is plotted (lower panel). The upper panel shows the spectrum on the disk, with three strong absorption lines due to the fundamental band of CO. In the lower part of the upper frame the location of the limb is plotted as a function of wavelength. Note how the strong CO lines extend above the continuum limb to heights traditionally occupied by the chromosphere. Such data and analyses, carried out by Solanki et al. (1994) and Ayres (2002), demonstrate that the very cool gas revealed by CO lines (Ayres et al. 1986) is really located at chromospheric heights.

Lack of space does not allow me to provide more details on these and other structures, nor to even scratch the surface of the vast literature dealing with them. The following monographs or reviews provide more detail, although none is very recent: Lites (1985), Bray & Loughhead (1974), Zirin (1996).

2. Chromospheric dynamics

Besides being strongly structured, the chromosphere is also extremely dynamic, showing both aperiodic and periodic variations. Of particular interest are the oscillatory
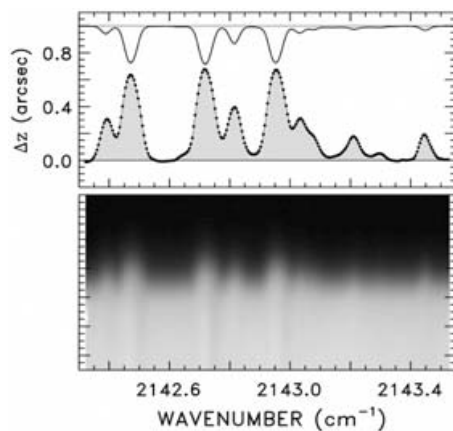
Figure 2. Lower frame: A part of the Sun's infrared spectrum along the spectrograph slit (vertical axis). Upper frame: spectrum on the disk (upper curve) and limb extension Δz (lower curve). Adapted from Ayres (2002).
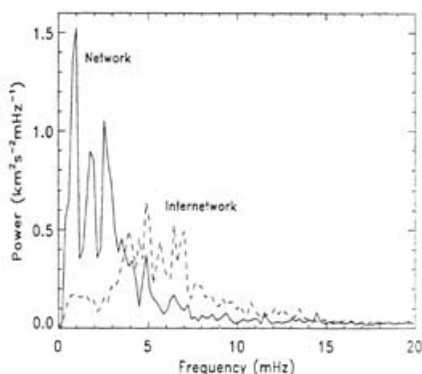

Figure 3. Velocity power spectra obtained in the quiet Sun with the Ca II H line, averaged separately over the network and internetwork (from Lites et al. 1993).

motions, which exhibit a far larger amplitude than their photospheric counterparts. These oscillations are seen in the cores of strong absorption lines, but also in EUV emission lines, and have a dominant period of 3 min, near the acoustic cutoff.

One of the most striking features of the chromospheric oscillations is that they differ significantly between the network (at the edges of supergranulation cells) and the internetwork (interiors of cells). In the internetwork the dominant period is three minutes. These waves are thought to be propagating upward (see Sect. 4; Carlsson & Stein 1997). Note, however, that a more complex picture is given by the intensity-velocity phase shifts and the phase differences between lines formed at different heights (e.g., Deubner & Fleck 1990). This is a major difference to photospheric oscillations, where the p-modes containing much of the oscillatory power are evanescent. A spatially averaged power spectrum of the oscillations found in the internetwork is indicated by the dashed line in Fig. 3, while the average power spectrum of network regions is indicated by the solid line. It is clear that neither feature shows a single sharp peak. The internetwork exhibits power mainly at a period of 3 min, but high power is found between 1.5 and 4 min, while the network exhibits power basically at periods longer than roughly 4-5 min (cf. Rutten & Uitenbroek 1991; Lites et al. 1993).

3. Chromospheric magnetism

The magnetic field in the chromosphere connects the coronal magnetic structures with their photospheric footpoints, i.e. it forms the transition from the photospheric flux tubes to the coronal loops and open field lines. This transition is far from trivial, involving magnetic canopies, cool and hot loops and strongly bent field lines. In addition, typically chromospheric structures such as prominences (Webb et al. 1998; Schmieder 1999) are produced when the magnetic field achieves a particular geometry. With high likelihood, spicules, Hα fibrils, etc. are also related to chromospheric magnetic fields (e.g., Sterling & Hollweg 1988).

One piece of evidence for the complexity of the chromospheric magnetic structure is provided by the moss, i.e. a cell-like pattern of bright material at nearly a million K. Superficially the moss looks like chromospheric plage, but a more careful analysis reveals that it does not correlate with the locations of photospheric magnetic flux. This suggests that the field lines are strongly bent on their way from the photosphere to the corona. Based on this, Berger et al. (1999) have proposed that magnetic loops are formed from combinations of field lines from many photospheric sources, i.e. from many photospheric flux tubes.

An ongoing debate centers on the role of magnetic canopies in the chromosphere, i.e. horizontal field overlying nearly field-free material. Canopies were introduced to explain the emission measures of chromospheric and transition region UV lines (Gabriel 1976). Measurements showed them to lie in the lower chromosphere, certainly in active regions (Giovanelli & Jones 1982), but also in the quiet Sun (Jones & Giovanelli 1983). It has recently been argued that no horizontal fields stronger than a fraction of a Gauss are present in the quiet chromosphere (Landi degl'Innocenti 1998) on the basis of scattering polarization measurements in the Na I D lines. Bianda et al. (1998, 1999), however, found strong evidence for horizontal, canopy-like fields on the basis of the Hanle effect shown by the Ca I 4227 Å and Sr II 4078 Å resonance lines. Theoretically, the presence of a canopy can be explained in the lower chromosphere if the atmosphere outside the flux tubes is cool, as expected from CO-clouds (Solanki & Steiner 1990). Schrijver & Title (2003) have pointed out that many of the field lines associated with the traditional canopy return to the photosphere near their parent flux tube, in contradiction to the idea of Gabriel (1976). This is probably correct (see Dowdy et al. 1986), but does not really argue against canopy-like magnetic structures (as defined above).

In general, the measurement of the magnetic field in the chromosphere by the Zeeman effect is made difficult by the fact that most Zeeman sensitive chromospheric lines are broad, optically thick and suffer from a complex line formation. Nonetheless, chromospheric magnetograms in H$_\beta$ have provided interesting results (see, e.g., Zhang & Zhang 2000). Radio observations provide the field strength near the base of the corona and have for a long time been nearly unique in this respect (e.g., White & Kundu 1997; Lee et al. 1999).

Fresh diagnostics, such as Hanle effect measurements in resonance lines (e.g. Stenflo 1994) or the He I 1083 nm triplet (formed in the upper chromosphere near the base of the corona) now provide information on the full magnetic vector. The He triplet has the advantage that its components are (generally) optically thin, narrow and magnetically sensitive. It does have a complex line formation, but for the measurement of the magnetic field this is not a serious drawback. With the help of a Stokes inversion code based on a genetic algorithm, it is possible to deduce the full magnetic vector with high accuracy close to the base of the corona (Lagg et al. 2004a). Such measurements have revealed a rich variety of often dynamic magnetic structures. Fig. 4 shows a map of the magnetic
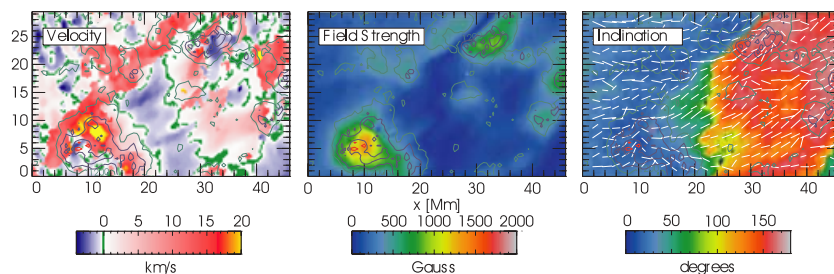
Figure 4. Maps of line of sight velocity (left panel), field strength (middle) and, in the right panel, magnetic inclination to the vertical (colours) as well as magnetic field azimuth (white lines) derived from Stokes vector measurements of the He I 1083 nm triplet. The image represents part of an emerging active region. The colour scales are given below each image.

vector and line of sight velocity in an emerging flux region (part of a young active region) obtained with the He I triplet. Note that the derived values do not all refer to the same height. The region with strong magnetic field near the lower left part of the image is a new-born pore that exhibits a strong downflow. A careful look at the line profiles located in this downflow region clearly reveals the presence of two independent magnetic components, one of which is nearly at rest, the other has a line-of-sight velocity of up to 40 km s^{-1} (see Lagg et al. 2004b for more details).

Another feature that is visible from this image is the gradual reversal of the magnetic polarity from the lower left ($\gamma \approx 0$) to the upper right ($\gamma \approx 180°$) corner, which outlines magnetic loops connecting these opposite polarities. The constant magnetic azimuth measured in this part of the image supports this interpretation. A more careful analysis confirms this interpretation (Solanki et al. 2003).

Finally, a particularly interesting structure is located near the top of the image, where a very abrupt polarity change occurs. This is best interpreted in terms of an electric current sheet, the first time that such a structure has been directly imaged on the Sun. Ohmic dissipation of magnetic energy can act at such locations. Current sheets are also preferred locations for magnetic reconnection (Priest 1999; Priest & Forbes 2000). They have been proposed as the locations of coronal heating through microflaring (Parker 1983a, b, 1988).

4. Models of the chromosphere

The standard model of the quiet solar chromosphere possesses a gentle temperature rise from the temperature minimum up to the base of the transition region, with temperatures always lying above 4000 K. Since the Sun is obviously not homogeneous, families of models, each member describing a different part of the chromosphere have been constructed. A widely used set of such models is the one produced by Fontenla et al. (1993). The various models in this set describe the internetwork regions (abbreviated as FALA), the average quiet Sun (FALC), the network (FALF) and active region plage (FALP). Basically, when going from lower to higher activity the temperature in the chromospheric layers increases. Such models reproduce many observational constraints, mainly time averaged (continuum and line) spectra in the UV and the visible.

A different approach has been taken by Carlson & Stein (1992, 1995, 1997). Their NLTE radiation MHD models are also one-dimensional, but dynamic, including the treatment of time-dependent excitations of atoms. A piston which moves in accordance with measured time series of photospheric vertical velocities provides the lower boundary
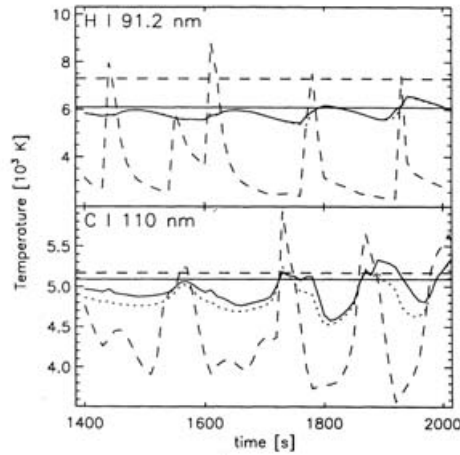
Figure 5. Radiation temperature of emitted intensity (solid) and electron temperature at $\tau_\nu = 1$ (dashed) as a function of time in a simulation. The solid and dashed straight lines are radiation temperature of averaged intensity and average of the Planck function, respectively (from Carlsson & Stein 1995).
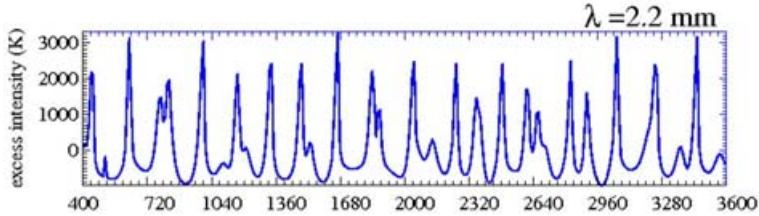

Figure 6. Intensity variations as a function of time (horizontal scale is in sec) computed at a wavelength of 2.2 mm for the Carlsson & Stein model (adapted from Loukitcheva et al. 2004a).

condition to the velocity. This piston drives waves that travel upwards, steepen as the density decreases with height and finally form shocks in the chromosphere. Attractions of this model are that it reproduces the time-dependent behaviour of the Ca II H and K lines and that cool gas is present between the shocks, as suggested by CO lines at 4.7 μm (see Sect. 1).

One of the important points made by Carlsson & Stein (1995) is that although the electron temperature in the middle and upper chromosphere, varies by well in excess of a thousand degrees over a wave period the radiation temperature and line intensities vary by much smaller amounts (in the range of hundreds of degrees). The time-averaged electron temperature in the Carlsson & Stein simulations keeps dropping with height and does not show a chromospheric temperature rise, in contrast to the 'standard' models of Fontenla et al. (1993). Temperature sensitive atomic chromospheric lines (e.g. the Ca K line core, or C I 110 nm) computed for the dynamic model, however, show strong emission, with comparatively low variability, mimicking spectra produced by a constantly hot chromosphere (see Fig. 5). The same is true for continua formed in truly chromospheric layers (see Fig. 5).

The dominance of shock waves in chromospheric layers is confirmed by the 3-D radiation hydrodynamic simulations of Wedemeyer et al. (2004). In this geometry the shock waves form a highly dynamic network-like pattern at the granulation scale. The limitations of this model lie therein that the radiative transfer is carried out in LTE, which breaks down at chromospheric heights due to the low gas density.

The Carlsson & Stein picture of the chromosphere has been criticised, mainly by Kalkofen and co-workers. They maintain that the Carlsson & Stein model is too cool in the intershock region at chromospheric layers. Although much of the criticism is based on relatively qualitative statements, Wilhelm & Kalkofen (2003) conclude from a careful study of data obtained by SUMER that the Lyman continuum exhibits temporal variations that are below 200 K in temperature units. The model, although predicting brightness variations that are almost an order of magnitude smaller than the variations in the electron temperature, still predicts temperature variations of around 500 K.

Further tests of these models have been made by Ayres (2002). A comparison with CO line observations led him to remark that the Carlsson & Stein models are not cool enough, i.e. he reached exactly the opposite conclusion as Kalkofen and co-workers. This demonstrates again just how incompatible the various diagnostics are and underlines the need for further advances in modelling. For example, none of the models discussed so far includes the effects of the magnetic field, in particular the magnetic canopy, which is expected to significantly influence the dynamics and the thermal structure of the atmosphere above the mid-chromosphere. The effect of magnetic flux tubes, which channel waves from the solar surface into the chromosphere (e.g. Ulmschneider & Musielak 2003) also needs to be taken into account.

In addition to such improvements in the models, greatly improved and sensitive diagnostics of the chromospheric structure and dynamics are needed. The missing diagnostic may be provided by time series of images at sub-mm and mm wavelengths. At these long wavelengths the Rayleigh-Jeans limit applies, so that intensity depends linearly on temperature. This comparatively weak dependence implies that such radiation samples both hot and cold gas (see Loukitcheva et al. 2004a). An illustration is given in Fig. 6, which shows the response of 2.2 mm radiation to a time series generated by Carlsson & Stein. Note the large amplitude of the observed oscillation compared to the radiation temperature in Fig. 5. In this sense mm wavelength radiation combines some of the advantages of the CO lines, which mainly see the cool gas, with those of atomic lines and UV continua, which mainly sample the hot gas.

Unfortunately, the sub-mm and mm data available in the literature suffer one serious disadvantage: the spatial resolution is exceedingly low. Hence, perhaps not surprisingly, the time averaged output of the Carlsson-Stein model and combinations of two FAL models (FALA and FALF) reproduce quiet Sun observations, although FALC alone does not. This shortcoming of the present data can only be overcome with interferometric methods and even then current instruments are limited to a frustratingly low spatial resolution. Nonetheless, interferometric observations carried out with the Berkeley–Illinois–Maryland–Array (BIMA) have provided the first observations of chromospheric oscillations at mm wavelengths and have led to new insights (see Loukitcheva et al. 2004b).

Further advances are expected from very recently carried out VLA observations, but the main breakthrough is expected from the Atacama Large Millimeter Array (ALMA), which will have sufficient spatial resolution to hopefully provide definitive answers to many of the open questions regarding the nature of the quiet chromosphere.

References

Ayres, T.R., Testerman, L., Brault, J.W. 1986, *Astrophys. J.* **304**, 542.

Ayres, T.R. 2002, *Astrophys. J.* **575**, 1104.

Berger, T.E., De Pontieu, B., Fletcher, L., Schrijver, C.J., Tarbell, T.-D., Title, A.M. 1999, *Sol. Phys.* **190**, 409.

Bianda, M., Solanki, S.K., Stenflo, J.O. 1998, *Astron. Astrophys.* **331**, 760.

Bianda, M., Stenflo, J.O., Solanki, S.K. 1999, *Astron. Astrophys.* **350**, 1060.

Bray, R.J., Loughhead, R.E. 1974, *The solar chromosphere*, Chapman and Hall, London.

Carlsson, M., Stein, R.F. 1992, *Astrophys. J. Lett.* **397**, L59.

Carlsson, M., Stein, R.F. 1995, *Astrophys. J. Lett.* **440**, L29.

Carlsson, M., Stein, R.F. 1997, *Astrophys. J.* **481**, 500.

Deubner, F.-L-, Flck, B. 1990, *Astron. Astrophys.* **228**, 506.

Dowdy, J. F., Rabin, D., Moore, R.L. 1986, *Sol. Phys.* **105**, 35.

Fontenla, J.M., Avrett, E.H., Loeser, R. 1993, *Astrophys. J.* **406**, 319.

Gabriel, A.H. 1976, *Royal Soc. London Philos. Trans. Series A* **281**, 339.

Giovanelli, R.G., Jones, H.P. 1982, *Sol. Phys.* **79**, 267.

Jones, H.P., Giovanelli, R.G. 1983, *Sol. Phys.* **87**, 37.

Lagg, A., Woch, J., Krupp, N., Solanki, S.K. 2004a, *Astron. Astrophys.* **414**, 1109.

Lagg, A., Woch, J., Krupp, N., Gandorfer, A., Solanki, S.K. 2004b, In *Multi-Wavelength Investi-gations of Solar Activity, Proc. IAU Symp. 213* (eds. E. Benevolenskaya et al.), Cambridge Univ. Press, Cambridge, in press.

Landi degl'Innocenti, E. 1998, *Nature* **392**, 256.

Lee, J., White, S.M., Kundu, M.R., Mikić, Z., McClymont, A.N. 1999, *Astrophys. J.* **510**, 413.

Lites, B.W. (Ed.) 1985, *Chromospheric Diagnostics and Modelling.* National Solar Observatory, Sunspot, NM.

Lites, B.W., Rutten, R.J., Kalkofen, W. 1993, *Astrophys. J.* **414**, 345.

Loukitcheva, M., Solanki, S.K., Carlsson, M., Stein, R.F. 2004a, *Astron. Astrophys.* **419**, 747.

Loukitcheva, M.A., Solanki, S.K., White, S. 2004b, In *Multi-Wavelength Investigations of Solar Activity, Proc. IAU Symp. 213* (eds. E. Benevolenskaya et al.), Cambridge Univ. Press, Cambridge, in press.

Parker, E.N. 1983a, *Astrophys. J.* **264**, 635.

Parker, E.N. 1983b, *Astrophys. J.* **264**, 642.

Parker, E.N. 1988, *Astrophys. J.* **330**, 474.

Priest, E.R. 1999, *Astrophys. Space Sci.* **264**, 77.

Priest, E.R., Forbes, T. 2000, *Magnetic reconnection: MHD theory and applications*, Cambridge Univ. Press, New York.

Rutten, R.J., Uitenbroek, H. 1991, *Sol. Phys.* **134**, 15.

Schmieder, B. 1999, In *Solar and Stellar Activity: Similarities and Differences (eds. C.J. Butler, J.G. Doyle),* ASP Conf. Ser. 158, 133.

Schrijver, C.J., Title, A.M. 2003, *Astrophys. J. Lett.* **597**, L165.

Solanki, S.K., Steiner, O. 1990, *Astron. Astrophys.* **234**, 519.

Solanki, S.K., Livingston, W., Ayres, T. 1994, *Science* **263**, 64.

Solanki, S.K., Lagg, A., Woch, J., Krupp, N., Collados, M. 2003, *Nature* **425**, 692.

Stenflo, J.O. 1994, *Solar magnetic fields: polarized radiation diagnostics,* Kluwer Academic Pub-lishers, Dordrecht.

Sterling, A.C., Hollweg, J.V. 1988, *Astrophys. J.* **327**, 950.

Ulmschneider, P., Musielak, Z. 2003, In *Current Theoretical Models and Future High Resolution Solar Observations: Preparing for ATST,* ASP Conf. Ser. 286, 363.

Webb, D.F., Schmieder, B., Rust, D.M. (Eds.) 1998, *IAU Colloq. 167: New Perspectives on Solar Prominences,* ASP Conf. Ser. 150.

Wedemeyer, S., Freytag, B., Steffen, M., Ludwig, H.-G., Holweger, H. 2004, *Astron. Astrophys.* **414**, 1121.

White, S.M., Kundu, M.R. 1997, *Sol. Phys.* **174**, 31.

Wilhelm, K., Kalkofen, W. 2003 *Astron. Astrophys.* **408**, 1137.

Zhang, H., Zhang, M. 2000, *Sol. Phys.* **196**, 269.

Zirin, H. 1996, *Sol. Phys.* **169**, 313.